Non-Linear Analysis of Adhesive Joints in Composite Structures

E. Selahi*
Department of Mechanical Engineering, Marvdasht Branch
Islamic Azad University, Marvdasht, Iran
E-mail: ehsan.selahi@gmail.com
*Corresponding author

M.H. Kadivar
School of Mechanical Engineering,
University of Shiraz, Iran

Abstract: This paper presents a novel formulation and numerical solutions for adhesively bonded composite joints with non-linear (softening) adhesive behaviour. The presented approach has the capability of choosing arbitrary loadings and boundary conditions. In this model adherends are orthotropic laminates that obey classical lamination theory. The stacking sequences can be either symmetric or asymmetric. Adhesive layer(s) is (are) homogenous and isotropic material. They are modeled as continuously distributed non-linear (softening) tension/compression and shear springs. In this method by employing constitutive, kinematics and equilibrium equations, sets of differential equations for each inside and outside of overlap zones are derived. In the inside of overlap zone, the set of differential equations is non-linear, that is solved numerically. By solving these equations, shear and peel stresses in adhesive layer(s) as well as deflections, stress resultants and moment resultants in the adherends are determined. Most of adhesives have non-linear behavior, therefore unlike previous methods, in which the adhesive layers are modeled as linear materials, in the presented approach the non-linear behavior is assumed for the adhesive layer and can be used to analyze the most of adhesive joints. The numerical results reveal that in the inside of overlap zone, magnitudes of shear forces are considerably large due to high rate of variation in the bending moments. The developed results are successfully compared with those obtained by finite element analysis using ANSYS. The comparisons demonstrate the accuracy and effectiveness of the aforementioned methods.

Biographical notes: E. Selahi received his PhD in Mechanical Engineering from Ferdowsi University of Mashhad in 2013. He is currently Assistant Professor at the Department of Mechanical Engineering, Islamic Azad University, Marvdasht Branch, Marvdasht, Iran. His current research interest includes Composite Structures, Joints and Biomechanics.

1   INTRODUCTION

Wide existing and potential applications of composite materials such as: light weight, high specific strength and stiffness, vibration damping, corrosion resistance, impact resistance and ease of fabrication, maintenance and repair leads to use them intensively over recent decades in various sectors of industries. Joining different parts of composite structures can be achieved by using, bolted or bonded joints. Despite the fact that bolted joints, often suffer from high stress concentration and tendency of tearing through the holes. Since adhesive joints offer significant advantages over traditional fastening joining methods such as: improving the stress distribution, capability of joining and sealing simultaneously, and providing bonding wide range of different thicknesses of adherends, they are the most suitable joints for composite structures. Performances of adhesive joints are influenced severely by types of joints. Some of popular types of adhesive joints are: single lap, double lap, double strap and single scarf [1].

The first attempt for analyzing adhesive joints was carried out by Volkersen [2], He studied an adhesively bonded single-lap joint, in which the adhesive layer was modeled as continuous shear springs. In his model, the effects of bending moment caused due to eccentricity of loading axes were ignored. This model was modified by Goland et al. [3]. They described adhesive layer in terms of uniformly distributed transverse normal and shear springs. Most research on the analysis of adhesive joints has been performed by Hart-Smith [4] to [6] who presented some methods to investigate the structural responses of various types of adhesive bonded joints.

In all researches mentioned above, adherends are homogeneous and isotropic materials. Mortensen et al. [7] analyzed the single lap adhesive joint with generally orthotropic laminates. In this model adhesive layer is continuously has distributed the linear tension/ compression and shear springs. This model solved numerically. Selahi et al. [8] to [12] investigated some common and uncommon adhesively bonded composite joints, and studied the influences of geometrical dimensions and the spew fillets at boundaries of the joint. All of these models assumed to have linear behavior. These models are solved analytically.

Most of adhesives have non-linear behavior and the problem of adhesive joints with non-linear material behavior is a fundamental problem in joining analysis. Therefore the aforementioned review motivated us to present an efficient non-linear method for analyzing composite adhesive joint with non-linear behavior in their adhesive layer(s) subjected to in-plane loadings.

2   THEORETICAL DEVELOPMENT

Non-linear mathematical modeling of adhesive joints is obtained by adopting sets of restrictive assumptions for description the behavior of bonded joints. Based on these assumptions, constitutive and kinematics relations for each of adherends and constitutive relations for adhesive layer(s) are obtained. By combining these relations and equations, governing equations in the form of a system of differential equations, for each zone (inside and outside of overlap zone) are obtained. In the inside of overlap zone, the governing equations are non-linear. Assumptions for the adherends, adhesive layers, loading and boundary conditions are as follows:

- Adherends:
    - ✓ Adherends are modelled as wide beams.
    - ✓ Adherends are orthotropic laminates that obey special case of classical lamination theory.
    - ✓ The laminates are assumed to obey linear elastic constitutive laws.
    - ✓ Strains are small and rotations are very small.

- Adhesive layers:
    - ✓ Adhesive layer(s) is (are) assumed to behave as homogenous, isotropic and non-linear elastic material(s). Adhesive layer(s) are modelled as continuously distributed non-linear (softening) tension\compression and shear springs.

- Loading and boundary condition:
    - ✓ Loading and boundary conditions are arbitrary.

In Figs. 1 to 4, single lap, double lap, double strap and single scarf adhesive joints models that are subjected to different loadings at the ends are shown as follows:

N_x : Extensional resultant force

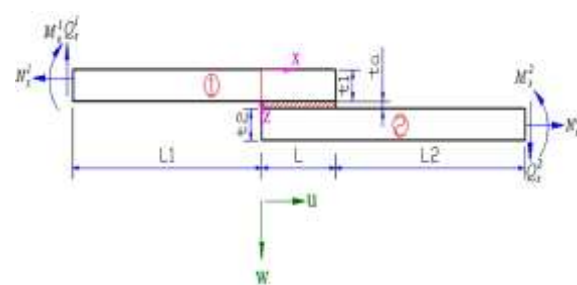Q_x : Shear resultant force

M_x : Bending resultant force

Fig. 1   Single lap adhesive joint
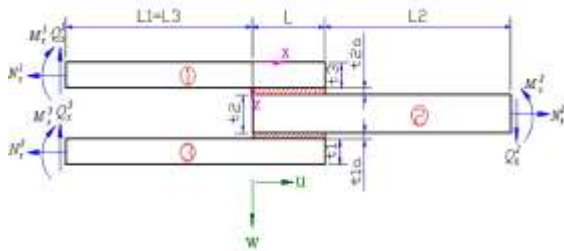
Fig. 2   Double lap adhesive joint

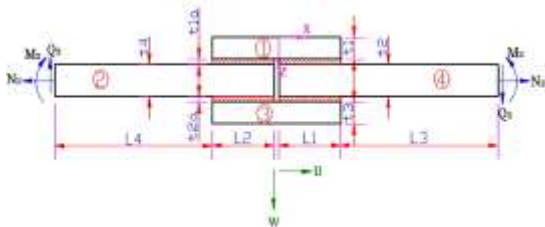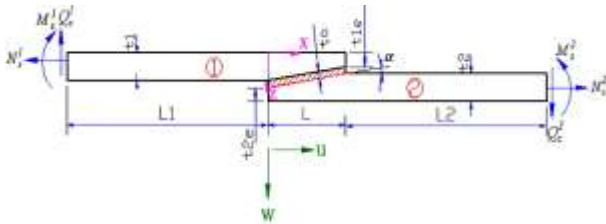**Fig. 3**   Double strap adhesive joint

Fig. 4   Single Scarf adhesive joint

The thicknesses of adherends in the single lap, double lap and double strap joints, are constant as follows:

$$t_1(x) = t_1$$
$$t_2(x) = t_2 \qquad (1)$$
$$t_3(x) = t_3$$

In the single scarf joint, the thickness of adherends are variable and defined as Eq. (2):

$$t_1(x) = t_1 - \frac{t_1 - t_1 e}{L} x$$
$$t_2(x) = t_{2e} - \frac{t_{2e} - t_2}{L} x \qquad (2)$$

In the modelling of adherends as wide beams, the transverse displacement is ignored. Also in the classical lamination theory, ε_z is assumed to be zero [13], so that displacement vectors are only functions of horizontal coordinate, (x).

$$u_0^i = u_0^i(x)$$
$$w^i = w^i(x) \qquad (3)$$

Where: u_0^i is a mid-plane axial displacement and w^i is a through thickness displacement in i-th layer (i=1, 2 or 3). So that classical lamination theory is simplified to [1]:

$$N_x^i = A_{11}^i u_{0,x}^i - B_{11}^i w_{,xx}^i$$
$$M_x^i = B_{11}^i u_{0,x}^i - D_{11}^i w_{,xx}^i \qquad (4)$$

Also kinematic relations for adherends are as Eq. (5) [1]:

$$u^i = u_0^i - z \beta_x^i$$
$$w_{,x}^i = \beta_x^i \qquad (5)$$

By considering Eqs. (4) and (5), Eqs. (6) and (7) are derived as follow [8]:

$$u_{0,x}^i = \frac{D_{11}^i N_x^i - B_{11}^i M_x^i}{A_{11}^i D_{11}^i - B_{11}^{i\,2}} \qquad (6)$$

$$\beta_{,x}^i = \frac{B_{11}^i N_x^i - A_{11}^i M_x^i}{A_{11}^i D_{11}^i - B_{11}^{i\,2}} \qquad (7)$$

In this paper, adhesive layer(s) are modelled as continuously distributed non-linear (softening) tension\compression and shear springs. In this modelling, shear and peel stresses in the adhesive layer(s) is (are) determined by Eqs. (8) and (9).

$$\sigma = a\varepsilon - b\varepsilon^3 = a(\frac{w^i - w^j}{t_a}) - b(\frac{w^i - w^j}{t_a})^3 \qquad (8)$$

$$\tau = c\gamma - d\gamma^3 = c(\frac{u^i - u^j}{t_a}) - d(\frac{u^i - u^j}{t_a})^3 =$$
$$c(\frac{u_0^i + \frac{t_i(x)}{2}\beta^i - u_0^j + \frac{t_j(x)}{2}\beta^j}{t_a}) - d(\frac{u_0^i + \frac{t_i(x)}{2}\beta^i - u_0^j + \frac{t_j(x)}{2}\beta^j}{t_a})^3 \qquad (9)$$

Equilibrium equations in the adhesive joints are different in the outside and inside of overlap zones. General forms of equilibrium equations, in the outside of overlap zones are the same for all types of adhesive joints. In Fig. 5, an equilibrium element in the outside of overlap zone is shown.
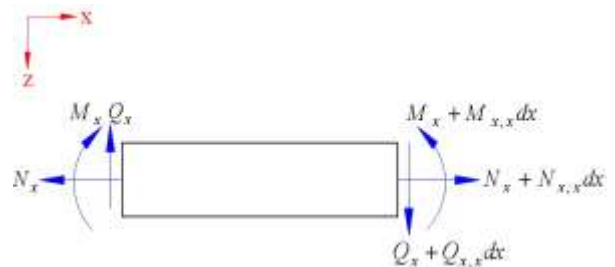

Fig. 5   Equilibrium element in the outside of overlap zones

So that the equilibrium equations in the outside of overlap zone are as follows [9]:

$$N_{x,x}^i = 0 \Rightarrow N_x^i = Const \qquad (10)$$

$$Q_{x,x}^i = 0 \Rightarrow Q_x^i = Const \tag{11}$$

$$M_{x,x}^i = Q_x^i \Rightarrow M_x^i = Q_x^i x + Const \tag{12}$$

Equilibrium equations in the inside of overlap zone are different for each type of adhesive joints. In this modelling, each equilibrium element in the inside of overlap zone consists of an element of adherend with half thickness of adhesive layer(s). In Fig. 6, equilibrium elements in the inside of overlap zone for single lap adhesive joint are shown.
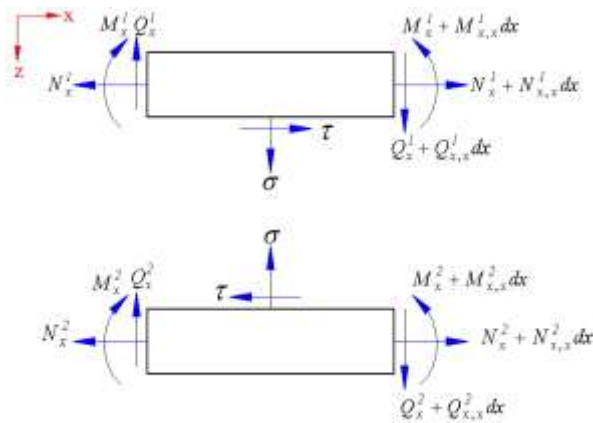

Fig. 6   Equilibrium elements in the inside of overlap zone for single lap joint
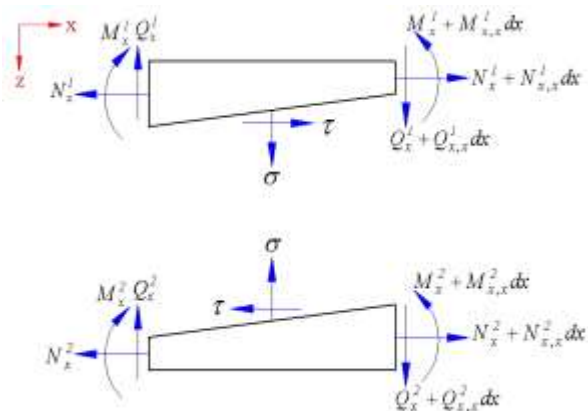

Fig. 7   Equilibrium elements in the inside of overlap zone for single scarf joint

So that: for this joint, equilibrium equations in the inside of overlap zone are as Eq. (13) [7].

$$N_{x,x}^1 = -\tau$$
$$Q_{x,x}^1 = -\sigma$$
$$M_{x,x}^1 = Q_x^1 - \tau \frac{t_1 + t_a}{2}$$
$$N_{x,x}^2 = \tau \tag{13}$$
$$Q_{x,x}^2 = \sigma$$
$$M_{x,x}^2 = Q_x^2 - \tau \frac{t_2 + t_a}{2}$$

In Fig. 7, equilibrium elements in the inside of overlap zone for single scarf adhesive joint are shownSo that: for this joint, equilibrium equations in the inside of overlap zone are as Eq. (14) [10].

$$N_{x,x}^1 = -\tau$$
$$Q_{x,x}^1 = -\sigma$$
$$M_{x,x}^1 = Q_x^1 + N_x^1 \tan \frac{\alpha}{2} - \tau \frac{t_1(x) + \dfrac{t_a}{\cos \alpha}}{2}$$
$$N_{x,x}^2 = \tau \tag{14}$$
$$Q_{x,x}^2 = \sigma$$
$$M_{x,x}^2 = Q_x^2 + N_x^2 \tan \frac{\alpha}{2} - \tau \frac{t_2(x) + \dfrac{t_a}{\cos \alpha}}{2}$$

In Fig. 8, equilibrium elements in the inside of overlap zone for double lap and double strap adhesive joints are shown.
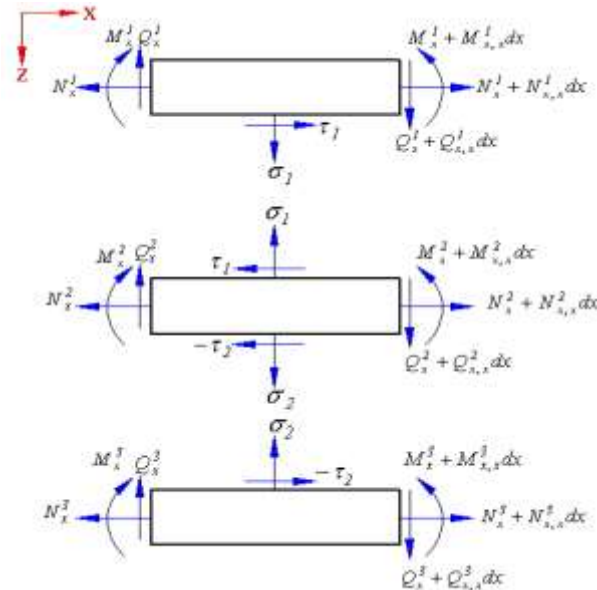

Fig. 8   Equilibrium elements in the inside of overlap zone for double lap and double strap joints

So that: for these joints, equilibrium equations in the inside of overlap zone are shown as Eq. (15) [8].

$$N^1_{x,x} = -\tau_1$$

$$Q^1_{x,x} = -\sigma_1$$

$$M^1_{x,x} = Q^1_x - \tau_1 \frac{t_1 + t_a}{2}$$

$$N^2_{x,x} = \tau_1 - \tau_2$$

$$Q^2_{x,x} = \sigma_1 - \sigma_2 \qquad (15)$$

$$M^2_{x,x} = Q^2_x - (\tau_1 - \tau_2)\frac{t_2 + t_a}{2}$$

$$N^3_{x,x} = \tau_2$$

$$Q^3_{x,x} = \sigma_2$$

$$M^3_{x,x} = Q^3_x - \tau_2 \frac{t_3 + t_a}{2}$$

By combining constitutive and kinematic relations in adherends and adhesive layer(s) with equilibrium equations in the inside and outside of overlap zones, sets of differential equations are derived. In the outside of overlap zone, the governing equations are six differential equations as follows [9]:

$$N^i_{x,x} = 0 \Rightarrow N^i_x = C_1 \qquad (16)$$

$$Q^i_{x,x} = 0 \Rightarrow Q^i_x = C_2 \qquad (17)$$

$$M^i_{x,x} = Q^i_x \Rightarrow M^i_x = C_2 x + C_3 \qquad (18)$$

$$u^i_{0,x} = \frac{D^i_{11} N^i_x - B^i_{11} M^i_x}{A^i_{11} D^i_{11} - {B^i_{11}}^2} \qquad (19)$$

$$\beta^i_{,x} = \frac{B^i_{11} N^i_x - A^i_{11} M^i_x}{A^i_{11} D^i_{11} - {B^i_{11}}^2} \qquad (20)$$

$$w^i_{,x} = \beta^i \qquad (21)$$

In modelling of adhesive layer(s) in the forms of non-linear (softening) springs, the governing equations in the inside of overlap zone are sets of nonlinear differential equations. Here for the sake of brevity, only single lap adhesive joint is investigated. Governing equation in the inside of single lap adhesive joint is a set of 12 non-linear coupled differential equations as Eq. (22):

$$
\begin{cases}
u^1_{0,x} = \dfrac{D^1_{11} N^1_x - B^1_{11} M^1_x}{A^1_{11} D^1_{11} - {B^1_{11}}^2} \\[2mm]
\beta^1_{,x} = \dfrac{B^1_{11} N^1_x - A^1_{11} M^1_x}{A^1_{11} D^1_{11} - {B^1_{11}}^2} \\[2mm]
w^1_{,x} = \beta^1 \\[2mm]
N^1_{x,x} = -\tau = -c\left(\dfrac{u^2_0 + \frac{t_2(x)}{2}\beta^2 - u^1_0 + \frac{t_1(x)}{2}\beta^1}{t_a}\right) \\[2mm]
\qquad\quad + d\left(\dfrac{u^2_0 + \frac{t_2(x)}{2}\beta^2 - u^1_0 + \frac{t_1(x)}{2}\beta^1}{t_a}\right)^3 \\[2mm]
Q^1_{x,x} = -\sigma = -a\left(\dfrac{w^2 - w^1}{t_a}\right) + b\left(\dfrac{w^2 - w^1}{t_a}\right)^3 \\[2mm]
M^1_{x,x} = Q^1_x - \tau\dfrac{t_1 + t_a}{2} = Q^1_x + \left(-c\left(\dfrac{u^2_0 + \frac{t_2(x)}{2}\beta^2 - u^1_0 + \frac{t_1(x)}{2}\beta^1}{t_a}\right)\right. \\[2mm]
\qquad\qquad\left. + d\left(\dfrac{u^2_0 + \frac{t_2(x)}{2}\beta^2 - u^1_0 + \frac{t_1(x)}{2}\beta^1}{t_a}\right)^3\right)\dfrac{t_1 + t_a}{2} \\[2mm]
u^2_{0,x} = \dfrac{D^2_{11} N^2_x - B^2_{11} M^2_x}{A^2_{11} D^2_{11} - {B^2_{11}}^2} \\[2mm]
\beta^2_{,x} = \dfrac{B^2_{11} N^2_x - A^2_{11} M^2_x}{A^2_{11} D^2_{11} - {B^2_{11}}^2} \\[2mm]
w^2_{,x} = \beta \\[2mm]
N^2_{x,x} = \tau = c\left(\dfrac{u^2_0 + \frac{t_2(x)}{2}\beta^2 - u^1_0 + \frac{t_1(x)}{2}\beta^1}{t_a}\right) \\[2mm]
\qquad\quad - d\left(\dfrac{u^2_0 + \frac{t_2(x)}{2}\beta^2 - u^1_0 + \frac{t_1(x)}{2}\beta^1}{t_a}\right)^3 \\[2mm]
Q^2_{x,x} = \sigma = a\left(\dfrac{w^2 - w^1}{t_a}\right) - b\left(\dfrac{w^2 - w^1}{t_a}\right)^3 \\[2mm]
M^2_{x,x} = Q^2_x - \tau\dfrac{t_2 + t_a}{2} = Q^2_x + \left(-c\left(\dfrac{u^2_0 + \frac{t_2(x)}{2}\beta^2 - u^1_0 + \frac{t_1(x)}{2}\beta^1}{t_a}\right)\right. \\[2mm]
\qquad\qquad\left. + d\left(\dfrac{u^2_0 + \frac{t_2(x)}{2}\beta^2 - u^1_0 + \frac{t_1(x)}{2}\beta^1}{t_a}\right)^3\right)\dfrac{t_2 + t_a}{2}
\end{cases}
$$

$$(22)$$

3 NUMERICAL RESULTS AND DISCUSSIONS

In this section an example of single lap adhesive joint with fixed boundary condition in one side and the free boundary condition in the other side is considered. In plane, normal stress resultant $(N_x = 1 \times 10^4 \frac{N}{m})$ is applied at the free end, as shown in Fig. 9.
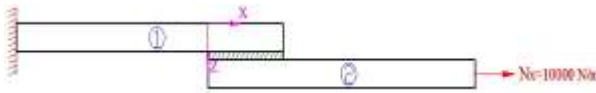
Fig. 9　　Loading and boundary condition in the sample

Dimensions of the specimen are coincided from ASTM D1002, standard test sample, which are shown in Fig. 10. The laminas of adherends are uni-directional fiberglass/epoxy. The adhesive layer is Epoxy DP 490. It behaves as a non-linear elastic material. Properties of this lamina are shown in table 1. The stacking sequences of both adherends are: $[0°, 45°, -45°, 90°]_{Sym}$.
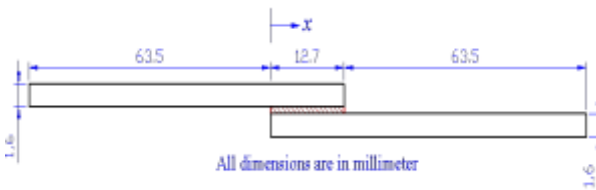
Fig. 10　　Dimensions of composite adhesive single lap joint in ASTM D1002

Table 1　　Properties of uni-directional fiberglass/epoxy lamina

	Material	Properties
Plies	Fiberglass/Epoxy	$E_1 = 36.8 \, GPa$, $E_2 = E_3 = 8.27 \, GPa$ $G_{12} = G_{13} = 4.14 \, GPa$, $G_{23} = 3 \, GPa$ $\nu_{12} = \nu_{13} = 0.26$, $\nu_{23} = 0.38$ $X = 450 \, MPa$, $Y = 31 \, Mpa$, $S = 72 \, MPa$, $t = 0.2 \, mm$

At first step, two curves in the forms of $\sigma = a\varepsilon - b\varepsilon^3$ and $\tau = c\gamma - d\gamma^3$ are fitted from peel stress-strain and shear stress-strain diagrams by linear regression. These curves are shown in Fig. 11. Poisons ratio for this adhesive is 0.4. At first the governing equations in the left outside of overlap zone are solved by using Eqs. (16) to (21) and by considering the boundary conditions in: $x = -63.5 \, mm$.
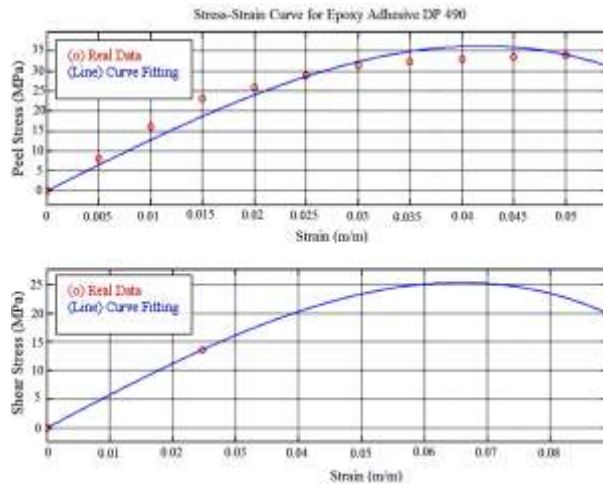
Fig. 11　　Normal stress-strain and shear stress-strain curves for Epoxy Adhesive DP 490

In the inside of overlap zone, the governing equations are non-linear Eq. set (22) and no analytic solution is existed. For solving these equations, a numerical method based on Runge Kutta 4th order is employed. The initial conditions are:

$$[u_0^1, \beta^1, w^1, N^1, Q^1, M^1, u_0^2, \beta^2, w^2, N^2, Q^2, M^2]_{x=0}$$

Three of these parameters are unknown and the others are known. The unknowns can be determined by try and error with Newton numerical method. For selecting good first guesses, these numbers are selected from the answers of linear solution of the governing equations (assume $\sigma = a\varepsilon$ and $\tau = c\gamma$). Then these first guesses are corrected by Newton Eq. (23). This try and error process is repeated until appropriate approximations are obtained. In Eq. (23), "i" subscript is used for these parameters at $x = 0$ and "f" is used for the parameters at $x = 0.0127 \, m$.

$$\begin{pmatrix} N_f^2 \\ Q_f^2 \\ M_f^2 \end{pmatrix} = \begin{pmatrix} \frac{\Delta N^2}{\Delta u_0^2} & \frac{\Delta N^2}{\Delta \beta^2} & \frac{\Delta N^2}{\Delta w^2} \\ \frac{\Delta Q^2}{\Delta u_0^2} & \frac{\Delta Q^2}{\Delta \beta^2} & \frac{\Delta Q^2}{\Delta w^2} \\ \frac{\Delta M^2}{\Delta u_0^2} & \frac{\Delta M^2}{\Delta \beta^2} & \frac{\Delta M^2}{\Delta w^2} \end{pmatrix} \begin{pmatrix} \Delta u_0^2 \\ \Delta \beta^2 \\ \Delta w^2 \end{pmatrix} + \begin{pmatrix} N_i^2 \\ Q_i^2 \\ M_i^2 \end{pmatrix} \quad (23)$$

By solving governing equations in the inside of overlap zone $u_0^1, \beta^1, w^1, Q^1, N^1, M^1, u_0^2, \beta^2, w^2$, N^2, Q^2 and M^2 in each point of inside overlap zone are determined. Then by using Eqs. (8) and (9), peel and shear stresses in each point of this zone are determined. Finally, the governing equations in the right outside of overlap zone are solved by using Eqs. (16)-(21) and by considering boundary conditions at: $x = -76.2 \, mm$.

Due to the lack of similar solution concerning the problem under consideration in the available literature, the present formulation and method of solution are validated by similar modeling obtained by finite element (FE) analysis using ANSYS. The sample is modelled by using 4640, 2D solid elements. Each element consists of 8 nodes.

In Fig. 12, the multi-linear stress-strain curve of the sample that is employed in the finite element modelling is shown. Each lamina of adherends is modelled by an orthotropic element through the thickness, and each adhesive layer is divided into two isotropic elements through the thickness. To get more accuracy, in the inside of overlap zone, meshes are finer than outside of overlap zones. In Fig. 13, the FE mesh model of this sample is shown.
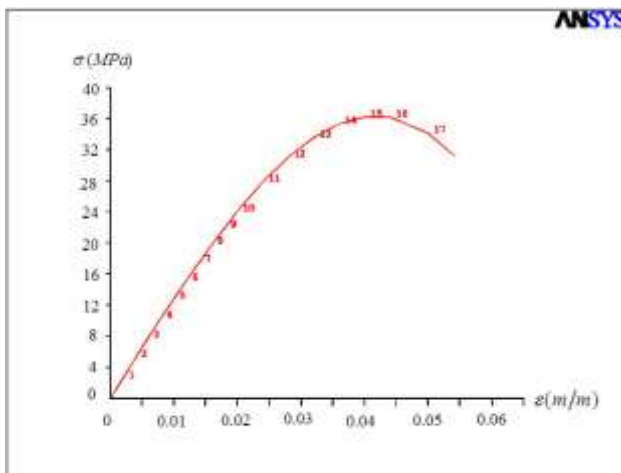
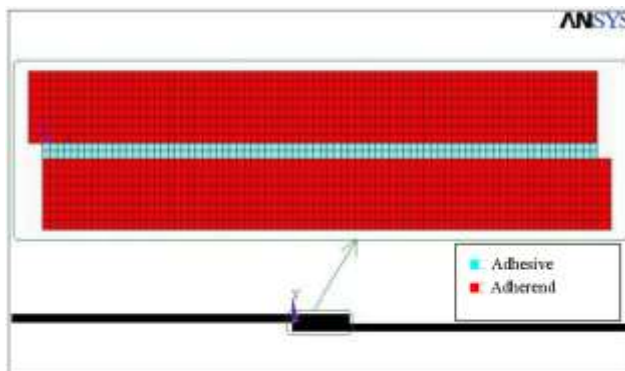**Fig. 12** Multi-linear stress- strain curve

Fig. 13 Multi-linear stress- strain curve

In the Figs. 14 to 17 diagrams of deflections, stress resultants and moment resultants of upper and lower adherends $(u_0^1, \beta^1, w^1, Q^1, N^1, M^1, u_0^2, \beta^2, w^2, N^2, Q^2, M^2)$ in each point of inside and outside of overlap zones are illustrated.
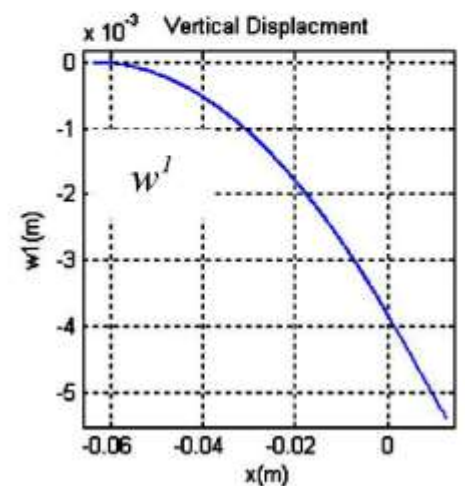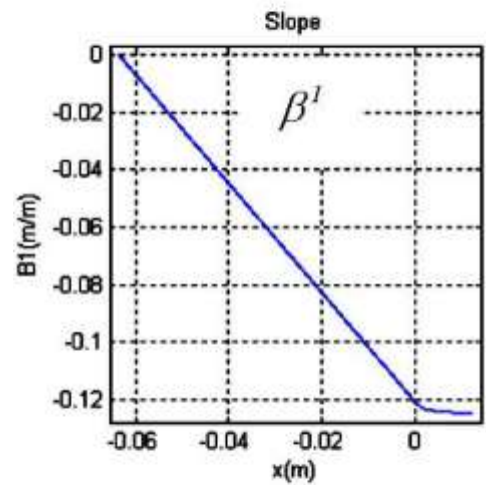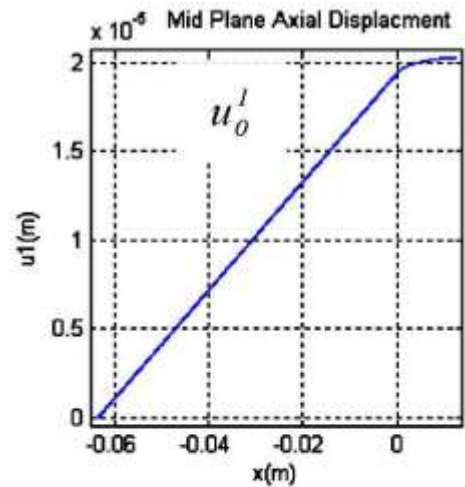
Fig. 14 Distributions of the u_0^1, β^1 and w^1 along the length of the overlap zone
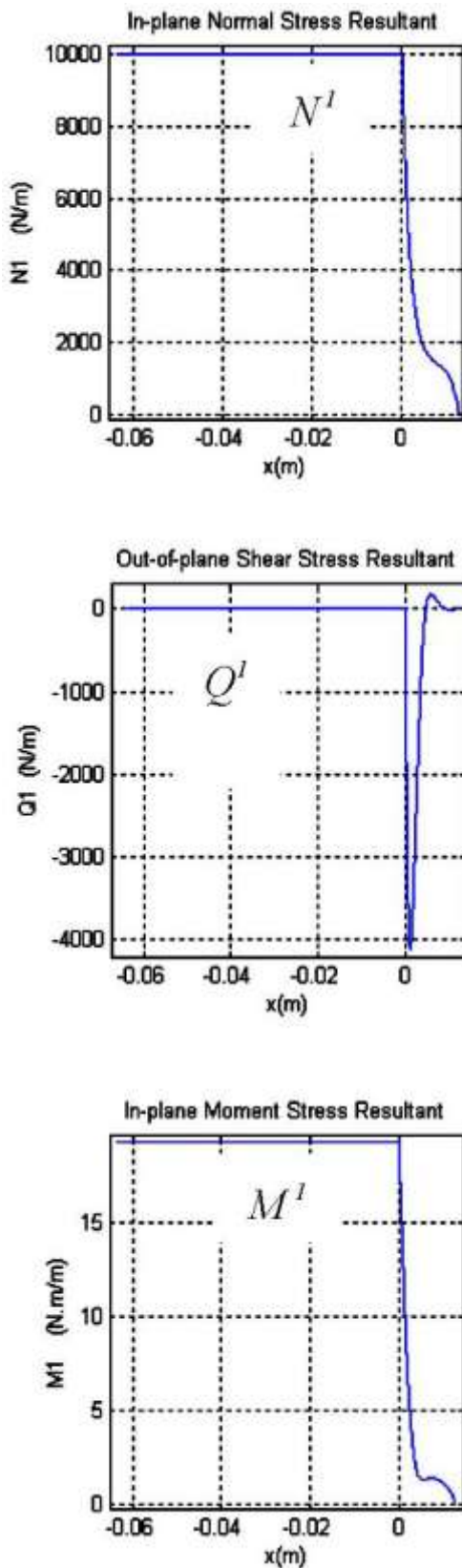
Fig. 15   Distributions of the N^1, Q^1 and M^1 along the length of the overlap zone

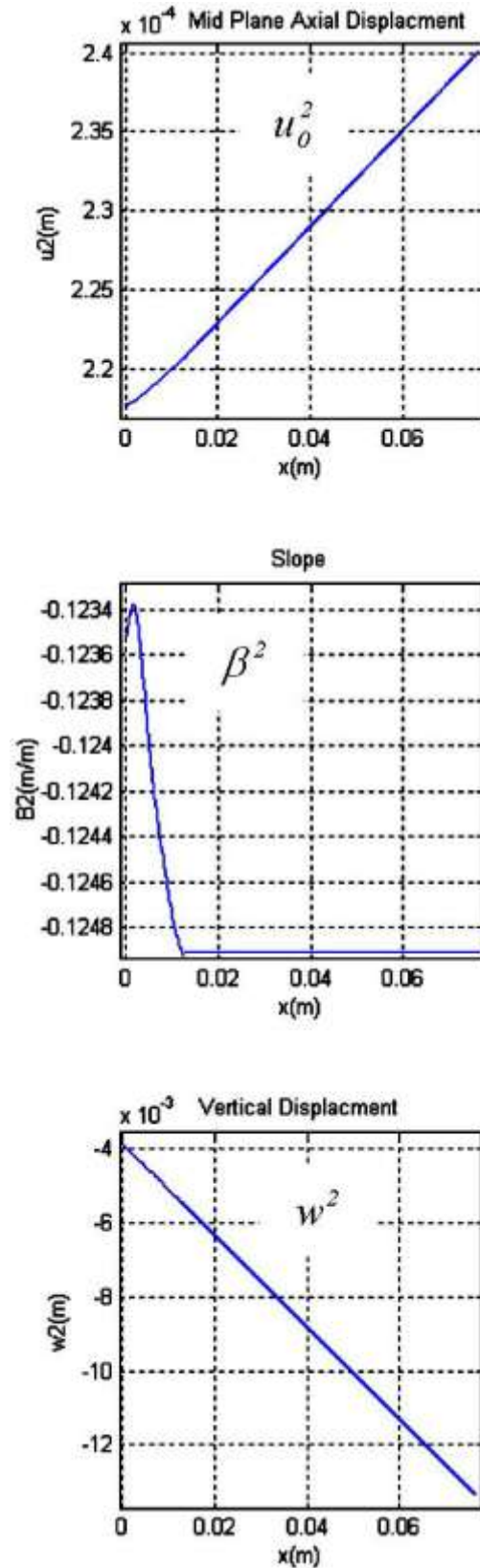**Fig. 16**   Distributions of the u_0^2, β^2 and w^2 along the length of the overlap zone

In-plane Normal Stress Resultant

N^2

Out-of-plane Shear Stress Resultant

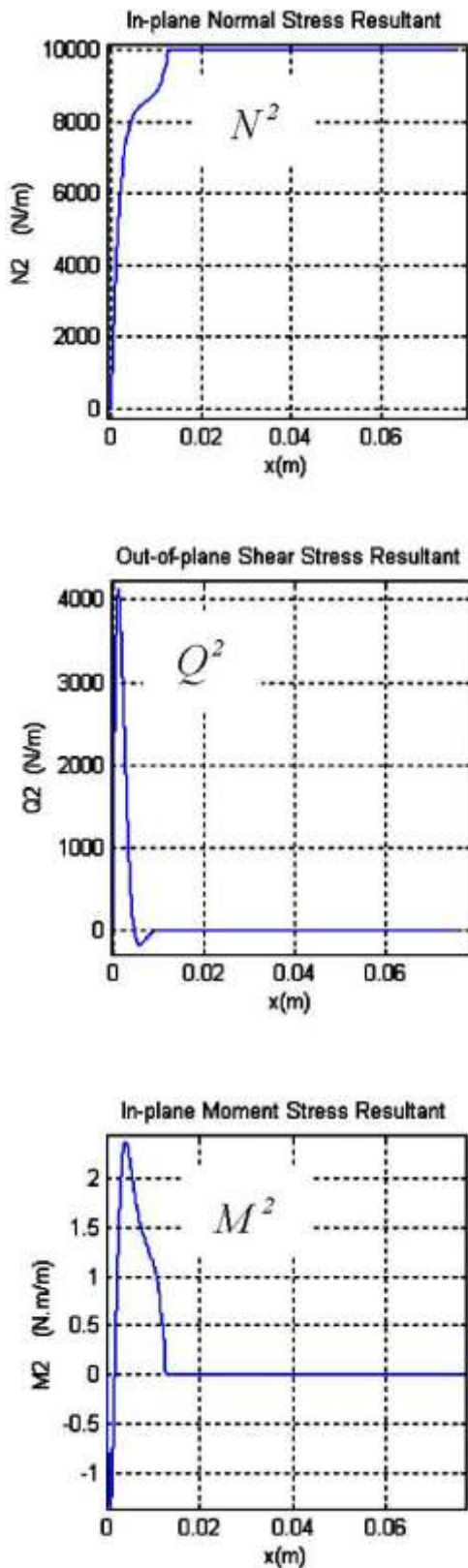Q^2

In-plane Moment Stress Resultant

M^2

Fig. 17   Distributions of the N^2, Q^2 and M^2 along the length of the overlap zone

In these figures it has been shown that: magnitudes of w^1, β^1, w^2 and β^2 are considerably large. This is due to eccentricity in the geometry of single lap adhesive joint, that generate significant bending moment in the adherends. The magnitudes of N^1 and N^2 in the outside of overlap zones are remain constant. In the inside of overlap zone, by increasing the magnitude of x, magnitude of N^1 is decreased and magnitude of N^2 is increased. It is because of force transmission from upper adherend to lower adherend.

It is seen that in the inside of overlap zone, it experience great magnitude of bending moment M^1 while the magnitude of bending moment M^2 is negligible. This is due to, creation of significant external bending moment in the left side boundary of upper adherend. In the inside of overlap zone, magnitudes of Q^1 and Q^2 are considerably large. This is due to high rate of variation in the magnitudes of their bending moments. Also due to the lack of shear forces in the adhesive joint, the diagrams of Q^1 and Q^2 are become symmetric. Figs. 18 and 19, depict the variation of peel and shear stresses along the length of overlap zone in the adhesive layer, for both non-linear mathematical approach and FE modeling.

By comparing between peel and shear stresses obtained from mathematical modelling and FE modelling, it is seen that the mathematical solutions shows a very good agreement with the results achieved from FE modeling that demonstrated the validity of the presented non-linear mathematical modelling. The loading path eccentricity in the single lap adhesive joints generates significant bending moment in the adherends that introduced high peel stress in the adhesive layer. Generally in the single lap adhesive joint and other asymmetric adhesive joints considerably high peel stresses are produced, that may cause failure in these adhesive joint types. The maximum peel and shear stresses in the adhesive layer are located at near the edges of overlap zone (x=0). This is due to high local bending moment in the upper adherend in this position.
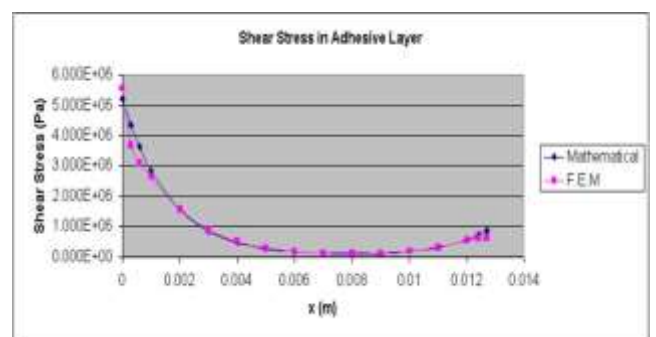

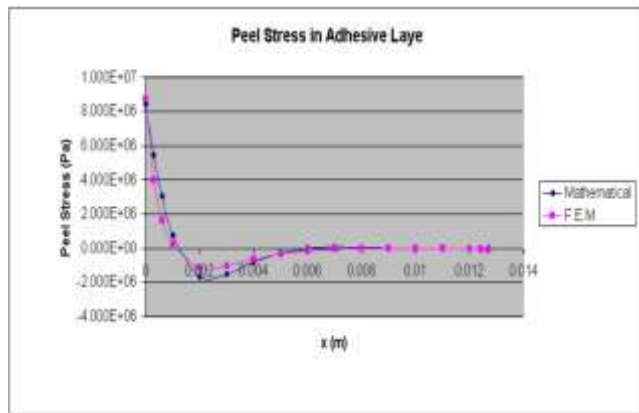**Fig. 18**   Shear stress distribution in adhesive layer

Fig. 19   Peel stress distribution in adhesive layer

4   CONCLUSION

Due to importance of the non-linear modelling of adhesive joints, an efficient numerical method is presented. In this paper adhesives are modelled as continuously distributed non-linear (softening) tension/compression and shear springs. Adherends have arbitrary stacking sequences and obeyed the classical lamination theory. It is found that the presented non-linear modeling yields accurate results when they were compared with the solutions of ANSYS software. The numerical results of the present method reveal the following conclusions:

a. In the single lap adhesive joints, magnitudes of slopes and deflections are considerably large. This is due to eccentricity in the geometry of this type of adhesive joint, which generates significant bending moment in the adherends.

b. In the inside of overlap zone, due to high rate of variation in the bending moments, magnitudes of shear forces are considerably large.

c. The loading path eccentricity in the single lap adhesive joints generates significant bending moment in the adherends that introduced high peel stress in the adhesive layer.

Most of adhesives have non-linear behaviour in their stress-strain curves. Therefore due to the high accuracy of the presented method, the developed results can be used as a benchmark for future researches of common types of adhesive joints that have non-linear behaviour in their adhesive layer(s).

REFERENCES

[1] Adams, R. D., Comyn, J., and Wake, W. C., Structural Adhesive Joints in Engineering, 2nd ed., Chapman & Hall, London, 1997, Chap. 2.

[2] Volkersen, O., "Die nietkraftverteilung in zugbeanspruchten niet ver bindungen mit konstanten lashenquers chnitten," Luftfahrt-Forschung, Vol. 15, 1938, pp. 41-47.

[3] Goland, M., and Reissner, E., "The stresses in cemented joints," Applied Mechanics, Vol. 15, 1944, pp. A17-A27.

[4] Hart-Smith, L. J., "Adhesive bonded scarf and stepped lap joints," Douglas Aircraft Company, NASA, CR 112235, 1973.

[5] Hart-Smith, L. J., "Adhesive bonded single lap joints," Douglas Aircraft Company, NASA, CR 112236, 1973.

[6] Hart-Smith, L. J., "Adhesive bonded double lap joints," Douglas Aircraft Company, NASA, CR 112237, 1973.

[7] Mortensen, F., and Thomsen, O. T., "Analysis of adhesive bonded joints: a unified approach," Composites Science and Technology, Vol. 62, 2002, pp. 1011-1031.

[8] Selahi, E., Rajabi, I., Behzadi, M., and Kadivar, M. H., "Analysis of adhesive double lap joint for composite materials," International Conference on Recent Advances in Composite Materials, Varanasi, India, 2004, pp. 232-235.

[9] Selahi, E., Rajabi, I., Jamali, M.J., and Kadivar M. H., "Analysis of adhesive double strap joint for composite materials," International Conference on Recent Advances in Composite Materials, Varanasi, India, 2004, pp. 208-213.

[10] Selahi, E., Rajabi, I., and Kadivar, M. H., "Mathematical modeling of composite single scarf adhesive joint," 13th International Mechanical Engineering Conference, Isfahan, Iran, 2005.

[11] Elahyari, S. M. R., Selahi, E., and Razi Mousavi S. H., "Geometry and loading condition effects on stress distributions of adhesive joint in composite structures," 14th International Mechanical Engineering Conference, Isfahan, Iran, 2006.

[12] Selahi, E., Tahani, M., and Yousefsani, S. A., "Analytical Solutions of Stress Field in Adhesively Bonded Composite Single-lap Joints under Mechanical Loadings," Journal of Engineering, Vol. 27, 2014, pp. 475-486.

[13] Jones, R. M., Mechanics of Composite Materials, 2nd ed., Script Book Company, Washington DC, 1975, Chap. 4.